# Chapter 4
# Electrochemical Behaviour of Solder Alloys

**C. Zou and C. Hunt**

## 4.1 Introduction

Achieving high reliability is a key issue in today's electronics assemblies, with a loss of continuity or short circuits failures, caused by metal corrosion an important failure mode. The corrosion source can originate from the manufacturing process, flux residues that may contain ionic or hydrophilic materials. Also operating in harsh environments where other aggressive species maybe encountered are another source of contaminants. Contaminants when combined with moisture result in a lowering of Surface Insulation Resistance (SIR) [1, 2] between conductors on the circuit and can accelerate corrosion. On a circuit assembly, corrosion may take place with and without the assistance of an applied voltage. Without the voltage bias, corrosion is driven by the electrochemical force, which depends thermodynamically on the anodic and cathodic processes. In general, the metals used for electronic circuit have a high corrosion resistance, without bias metal corrosion should not be a big concern. With applied bias, the voltage can overcome the electrochemical force driving further corrosion reactions to take place. In addition, the electric field on an insulating surface can also provide a driving force for metal ion migration and result in dendrite formation [3, 4]. Catastrophic failure occurs when dendrite growth between oppositely charged metal conductors bridge the conductor gap and cause short circuits, and is a very important failure mechanism in electronic assemblies.

A fundamental study of the electrochemical process that to dendrite formation is difficult, since the adsorbed atmospheric moisture layer is only approximately 100 nm thick. Typically, electrochemical studies use electrode systems that are on

C. Zou (✉) and C. Hunt
National Physical Laboratory, Hampton Road, Teddington,
Middlesex, TW11 0LW, UK
e-mail: ling.zou@npl.co.uk

G. Grossmann and C. Zardini (eds.), *The ELFNET Book on Failure Mechanisms, Testing Methods, and Quality Issues of Lead-Free Solder Interconnects*,
DOI: 10.1007/978-0-85729-236-0_4, 

a significantly greater dimensional scale than 100 nm. Dendrite formation is a three-step process. Firstly, metal is oxidized to metal ions into electrolyte, then metal ions migrate from the anode to cathode under an electric field, and finally metal ions are reduced to metal and deposited at the cathode. Clearly, all these processes are necessary for dendrite formation, and there are many factors that can influence these processes. *Metal oxidation at the anode*: each metal will have a different corrosion rate [5], and a metal with a fast corrosion rate will clearly form higher metal ion concentrations in the thin water film, hence enhancing the formation of dendrites. *Metal ion transportation*: if the metal ion forms an insoluble compound, it will not migrate from the anode to cathode, and therefore, solubility of the metal hydroxide is key to dendrite formation [6]. Finally, *metal deposition* at the cathode, Zamanzadeh [7] found that there is limiting over-potential for dendrite formation, below which dendrite formation can never occur. Most investigations have avoided such difficulties by using statistical evaluation of failures from SIR measurement, without addressing the electrochemical nature of potential failure processes. However, some researches on electrochemical corrosion of electronic metals are usually carried out in bulk solution without consideration of high ionic resistance between conductor lines on electronic circuits [8–11].

The conductor–insulator structure of a comb pattern with an adsorbed moisture layer is shown schematically in Fig. 4.1 and when an AC signal is applied an equivalent circuit representing each significant conduction process is also shown [12, 13]. $\boldsymbol{R_C}$ is the ionic resistance of the thin water layer with contaminants across the inter-electrode gap of the comb, and $\boldsymbol{C_C}$ is the capacitance of the comb pattern. The circuit elements in the dotted box $\boldsymbol{R_p}$ are a representation of electrochemical processes at the interface of the contaminant layer and electrode. These reactions represent the transition from electronic conduction in the electrode to ionic conduction in the contaminant layer. The equivalent circuit for these electrochemical processes includes the charge-transfer resistance $\boldsymbol{R_{CT}}$ associated with a faradic reaction at the electrode surface, $\boldsymbol{C_{DL}}$ a double layer or blocking capacitance at the interface, which may allow ionic current to flow in the absence of a faradic reaction, and $\boldsymbol{Z_W}$ the Warburg impedance, detectable when a faradic reaction occurs under diffusion control near the interface. The different conduction processes can be separated by electrochemical impedance (EI) measurements due to the different frequency dependences. EI results can separate ionic resistance $\boldsymbol{R_c}$ from overall impedance of the whole system ($\boldsymbol{R_T}$). This can provide the information on where the controlling step in the overall conduction process lies. In this conduction system, $\boldsymbol{R_C}$ is an important parameter, dominating metal corrosion and dendrite formation. In contrast, the SIR measurement can only measure the total resistance of the system.

The aim of this work was to investigate the corrosion of three solders and two PCB finish materials using EI. The two-electrode system of a comb test pattern, manufactured from the studied materials, was used and tested at an elevated temperature and humidity. The inter-electrode gap of 200 μm of the comb patterns reflected current high-density electronic circuit design. Dendrite formation was also assessed using SIR measurements, and these measurements were correlated

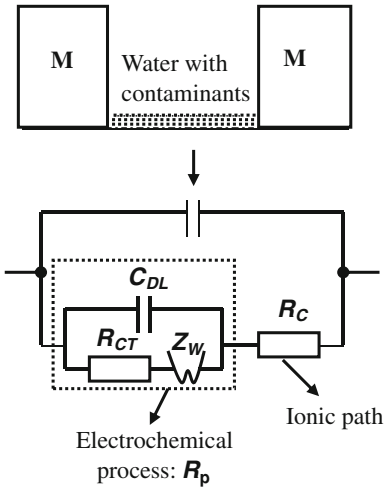


**Fig. 4.1** Conduction path for conductor–insulator structure

with the ionic resistance $R_C$. The applicability of using simple and quick non-destructive EI measurements to predict reliability was evaluated.

## 4.2 Experimental

### *4.2.1 Test Board*

A test board was designed consisting of four identical comb patterns, as shown in Fig. 4.2. The size of each comb pattern was 25 × 25 mm with 0.60 mm pitch and 0.20 mm gap. Boards were prepared with five finish materials: SAC, Sn, SnPb, ENIG and copper. Sn, ENIG and Cu-finished boards were obtained from the PCB supplier directly. SAC and SnPb finish boards were manufactured from Sn boards printed with proprietary no-clean solder pastes. The pastes used were $Sn_{63}Pb_{37}$ for the SnPb-finished boards and $Sn_{96.5}Ag_{3.0}Cu_{0.5}$ for the SAC-finished boards. Sn finish boards were used here to manufacture SAC and SnPb finish boards, the effect of underlying metal on the studied metal finish was therefore minimized, as solder may not completely wet the track surface particularly for SAC alloy. The wetting problem with the lead-free soldering process was found in a previous study [14].

### *4.2.2 Test Board Cleaning*

The aim of this work was to investigate the corrosion behaviour, and propensity of solder alloys and PCB finish materials to form dendrites. In order to eliminate any effects of contamination associated with the manufacture processes, the cleanliness

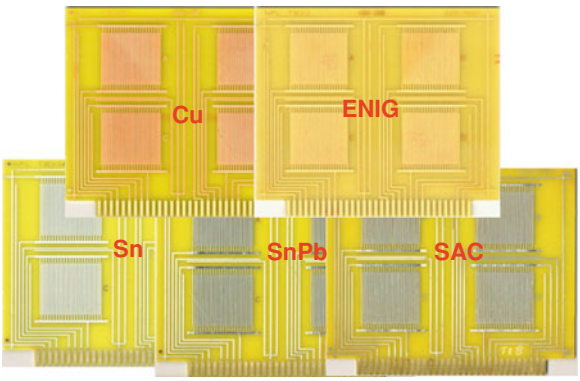


**Fig. 4.2** Test board with five finishes

of test boards with different finishes had not only to be assured but also to achieve similar high levels of SIR. The SAC and SnPb boards were prepared by printing onto the Sn finished as received boards with solder paste and reflowed before the following cleaning procedure. The cleaning procedures were as follows:

For the ENIG- and copper-finished boards:

Ionograph cleaning in 75% IPA + 25% DI water mixture at 45°C for 15 min

For Sn-finished board:

A single pass through a reflow process with a maximum temperature of 250°C
Ionograph cleaning in 75% IPA + 25% DI water mixture at 45°C for 15 min

For SAC-board and SnPb-finished board:

Ultrasonic cleaning in 100% Zestron FA + at 50°C for 5 min
DI water rinsing at 50°C for 5 min
Ionograph cleaning in 75% IPA + 25% DI water mixture at 45°C for 15 min

### *4.2.3 Test Flux*

A commercial flux was used for the study. The flux was recommended by a flux supplier and was a no-clean flux suitable for lead-free soldering. The flux was a low resin content, halide-free and solvent based.

### *4.2.4 Test Board Contamination*

The cleaned boards were fluxed using 50 μl of the test flux to cover each comb pattern. Fluxed boards were dried in a 100°C dry oven for 5 min for testing.

## 4.2.5 Flux Concentration

### 4.2.5.1 Electrochemical Impedance (EI) Measurements

For EI measurements, the flux was diluted to a certain level to achieve pronounced effects in the EI results from the electrochemical process. A dilution of 25% flux in IPA was used for all board finishes defined from the preliminary testing.

### 4.2.5.2 Surface Insulation Resistance (SIR) Measurement

For this work, it was necessary to determine the minimum flux concentrations that caused dendrite formation on the five board finishes. While this appears to be an artificial manipulation of the flux residue level, it does allow characterization of the flux residues in the critical regime for each board finish and is relevant since process residues vary over a wide range. Therefore, the flux concentrations were reduced as necessary from the as-received flux concentration by dilution with IPA. Three different concentrations (low, middle and high) were found for the different metal finishes from preliminary testing, and these are listed in Table 4.1.

## 4.2.6 Electrochemical Impedance (EI) Measurement

The EI was measured for each board finish using an ACM instruments GillAC. A two-electrode system was used for the test, as shown in Fig. 4.3. EI measurements were performed on three test patterns for ENIG board finish to check the repeatability of the test, and only one test pattern for the rest board finishes. As soon as the chamber reached the desired temperature and humidity, 40°C/93%RH, the open circuit potential (corrosion potential) was monitored for 60 minutes, then sample impedance were measured with the application of a 50mV peak-peak AC single with frequencies ranging from 3000 to 0.01 Hz.

## 4.2.7 Surface Insulation Resistance (SIR) Measurement

A single board, four test patterns, for each board finish was SIR tested. The SIR measurements were performed under the same condition as the EI measurements, 40°C/93%RH. A bias voltage of 5 V DC was applied during the test period of

**Table 4.1** Test flux concentration for different board finish

| Board finish | ENIG | Cu | SnPb | Sn | SAC |
|---|---|---|---|---|---|
| Flux concentration (% in IPA) | 5 | 50 | 15 | 15 | 15 |
| | 10 | 65 | 20 | 25 | 25 |
| | 15 | 80 | 25 | 35 | 35 |

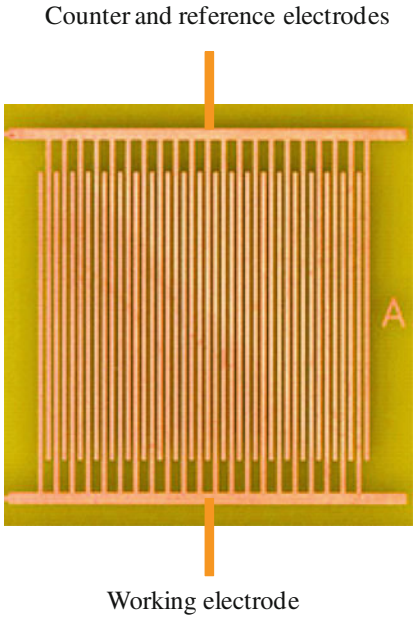


**Fig. 4.3** Two-electrode system for EI measurements

72 h, and the SIR was measured every 15 min. The test equipment had a $10^6$ Ω resistor incorporated into each test channel to preserve dendrite formation, so the minimum SIR measurement value of each channel was $10^6$ Ω.

### *4.2.8 EDX Analysis of Dendrites*

The dendrites formed during the SIR measurement on different board finish were identified and located using an optical microscope with back lighting, and the dendrite composition was assessed using an energy-dispersive X-ray (EDX) analyser attached to a SEM.

## 4.3 Results

### *4.3.1 Electrochemical Impedance Spectra on Five Board Finishes*

EI results, Bode, Nyquist and phase angle plots, for five board finishes are plotted in Figs. 4.4, 4.5, 4.6, 4.7 and 4.8. Three tests, A, B and C, were performed for the ENIG finish to check the repeatability of the testing. The results for three tests, as shown in Fig. 4.4, showed a reasonable good repeatability; hence, only one test was conducted for the rest board finishes.

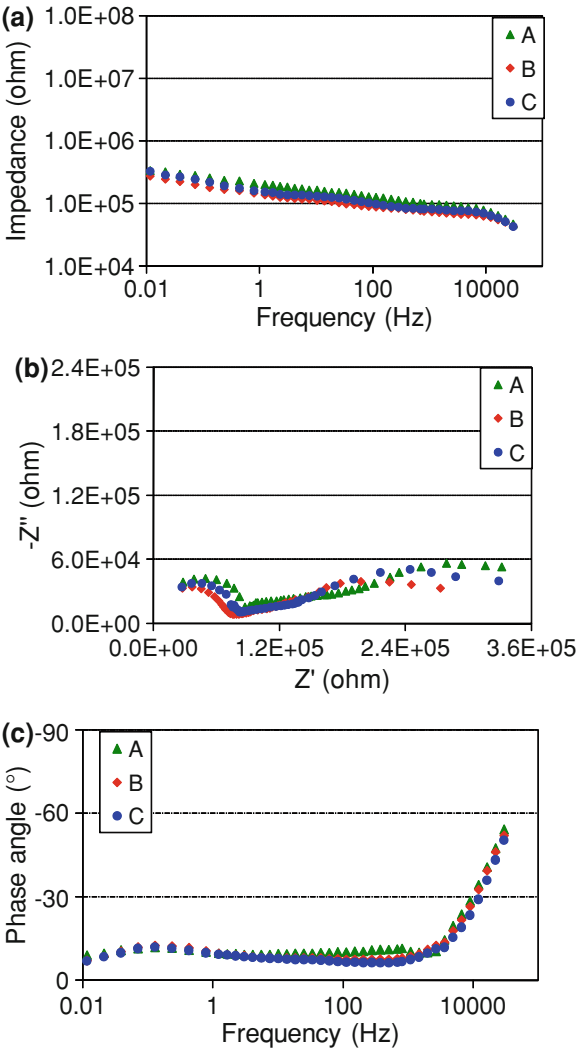


**Fig. 4.4** Bode, Nyquist and phase angle plots for ENIG board

The EI results for the different board finishes revealed a range of responses. For Sn, SAC and Cu board finishes, a single arc was observed in the Nyquist plot, demonstrating that the comb behaved as a simple parallel combination of $\boldsymbol{R_c}$ and $\boldsymbol{C_c}$ [12]. The components corresponding to electrochemical process were not pronounced in the results. Therefore, the $\boldsymbol{R_c}$ can be easily estimated as the diameter of the arc. In contrast, the electrochemical processes were clearly apparent in the Nyquist plot for ENIG and SnPb boards, as shown in Figs. 4.4 and 4.5. The first arc in the Nyquist plot was due to a parallel combination of $\boldsymbol{R_c}$ and $\boldsymbol{C_c}$, and the following behaviour in the plots represented mixed electrode reactions and diffusion processes, and correspond to the impedance components $\boldsymbol{R_{ct}}$, $\boldsymbol{C_{dl}}$ and $\boldsymbol{Z_w}$. A commonly observed second arc was not always seen in the plots due to a high $\boldsymbol{R_c}$, which

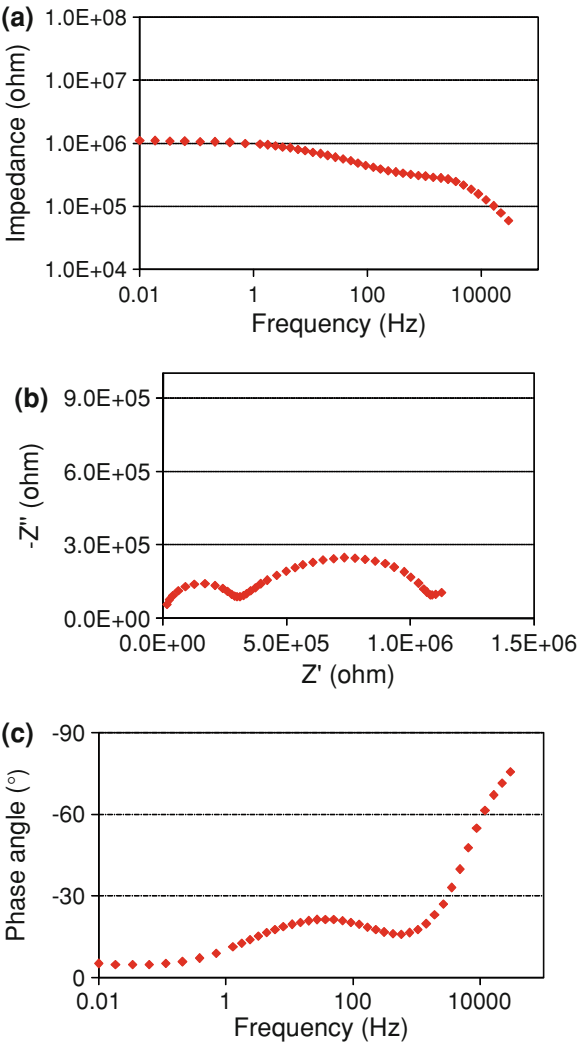


**Fig. 4.5** Bode, Nyquist and phase angle plots for SnPb board

also can be distorted due to the complication of the above processes. Therefore, these components are not always easy to interpret from the results. However, $\boldsymbol{R_c}$ always can be evaluated as the diameter of the first arc.

Another important parameter can be interpreted from the results is total impedance at low frequency (at 0.01 Hz). At the low frequency, the impedance measured from Bode plot is the overall resistance for all conduction processes. The impedance from capacitive components become negligible, and this is evidenced by the phase angle. The phase angle tends to 0° for all board finishes at 0.01 Hz.

The ionic resistances $\boldsymbol{R_c}$ evaluated from Nyquist plots and the total impedance at 0.01 Hz ($\boldsymbol{R_{p\ total\ (0.01)}}$) from Bode plots for the five studied metals are listed in

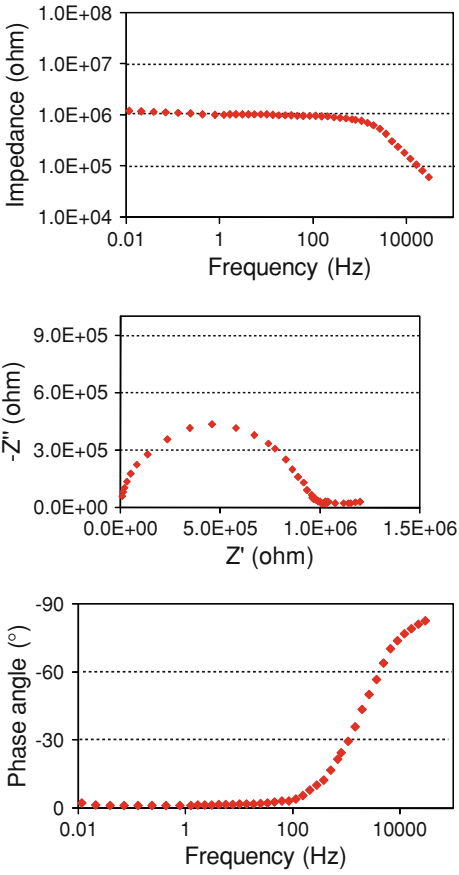


**Fig. 4.6** Bode, Nyquist and phase angle plots for SAC board

Table 4.2 and plotted in Fig. 4.9. These results show that the ionic resistance $\boldsymbol{R_c}$ dominates the overall impedance $\boldsymbol{R_{p\ total(0.01)}}$, as seen for Sn, SAC and Cu board finishes. At low ionic resistance, the impedance due to corrosion processes $\boldsymbol{R_p}$ becomes significant, as seen for SnPb and ENIG board finishes. Therefore, the lower ionic resistance of the system, the more pronounced the corrosion processes. The ranking from the highest to the lowest in terms of the ionic resistance is Cu > Sn ≈ SAC > SnPb > ENIG.

### *4.3.2 Surface Insulation Resistance Results*

The SIR values from four test patterns contaminated at three concentrations of flux for ENIG-finished boards are presented in Fig. 4.10 and those for SnPb, SAC, Sn and Cu-finished boards in Figs. 4.11, 4.12, 4.13 and 4.14, respectively.

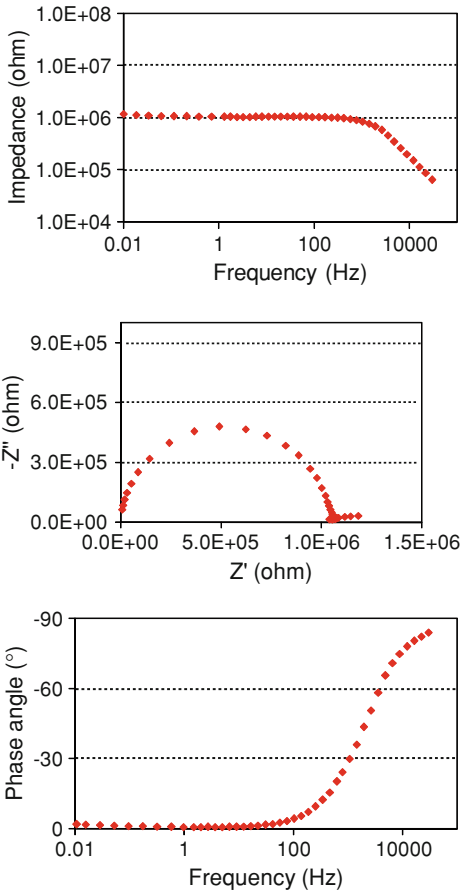


**Fig. 4.7** Bode, Nyquist and phase angle plots for Sn board

Some important findings should be noted from these results. For all board finishes at low flux concentrations, the SIR values slowly increased with time and stabilized within the test period. This increasing SIR was typical of the situation in which the ionic contaminants were depleted from the insulating surface due to mobile ions migrating towards the electrodes and then undergoing reduction and oxidation processes at both electrodes, and therefore no longer contributing to the conduction process. In the case of the intermediate flux concentration levels, occasional rapid changes in SIR values were noted, resulting from dendrite formation. Hence, this flux level was defined as the minimum flux concentration to promote dendrite (FCPD) growth. When the flux concentration was increased still further, dendrite formation was more prevalent, as shown by the third plot in each figure.

The FCPD are listed in Table 4.3 and plotted in Fig. 4.15 and the ranking for the resistance to dendrite formation is Cu > Sn ≈ SAC > SnPb > ENIG, similar to that of the ionic resistance $\boldsymbol{R_c}$ described earlier.

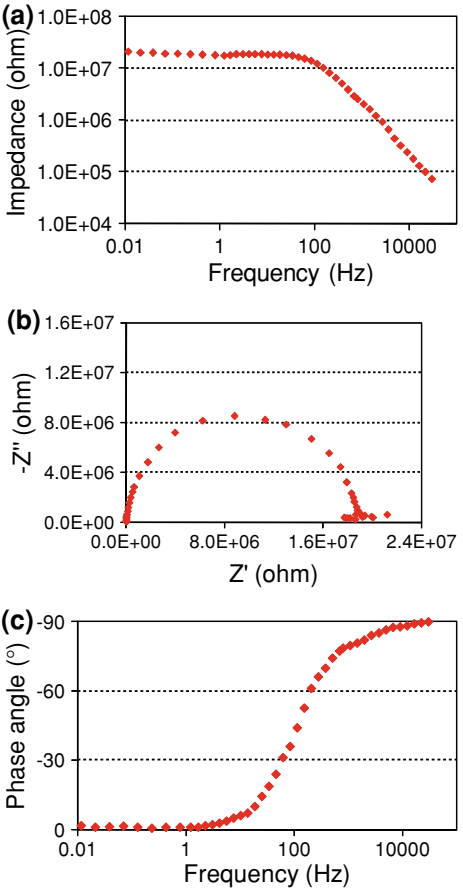


**Fig. 4.8** Bode, Nyquist and phase angle plots for Cu board

**Table 4.2** $R_{p\ total}$ and $R_c$ for five board finishes

| Metal | Cu | Sn | SAC | SnPb | ENIG |
|---|---|---|---|---|---|
| $R_{T(0.01)l}$ (MΩ) | 21.22 | 1.28 | 1.20 | 1.12 | 0.27 |
| $R_c$ (MΩ) | 20.11 | 0.98 | 0.92 | 0.34 | 0.07 |

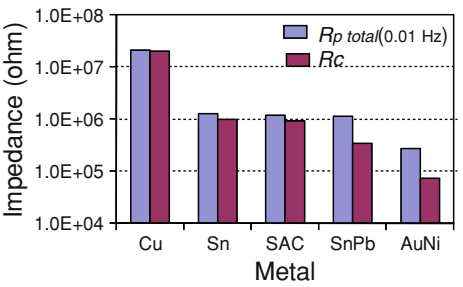


**Fig. 4.9** $R_{p\ total}$ and $R_c$ for five board finish boards

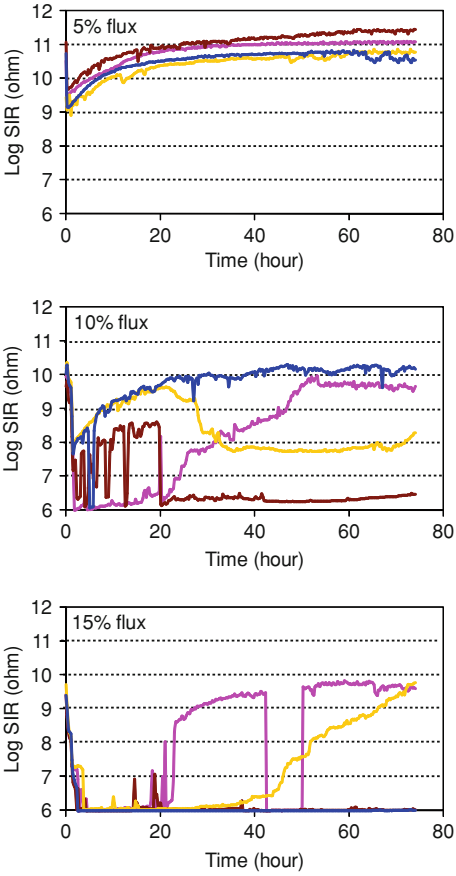


**Fig. 4.10** SIR results from ENIG boards with three concentrations of flux

### *4.3.3 SEM-EDX Analysis of Dendrites on SIR Boards*

The dendrites formed on different board finish during the SIR measurements were photographed using an optical microscope, as shown in Fig. 4.16, and analysed using SEM-EDX equipment. The results are listed in Tables 4.4, 4.5, 4.6, 4.7 and 4.8, and Figs. 4.17, 4.18, 4.19, 4.20 and 4.21. They are normalized and given in weight per cent. They revealed that for the ENIG-finished boards, the composition of the dendrites was mainly nickel, consistent (from an electrochemical point of view) with preferential dissolution of the nickel, compared with the noble metal gold.

On the copper-finished boards, the dendrites' composition was, as expected, 100% copper. However, for the SnPb board finish, the high Pb content in dendrites suggests that Pb is easier to corrode to form dendrite than Sn in SnPb alloy. On SAC board finish, the dendrites reflected the alloy composition and were mainly

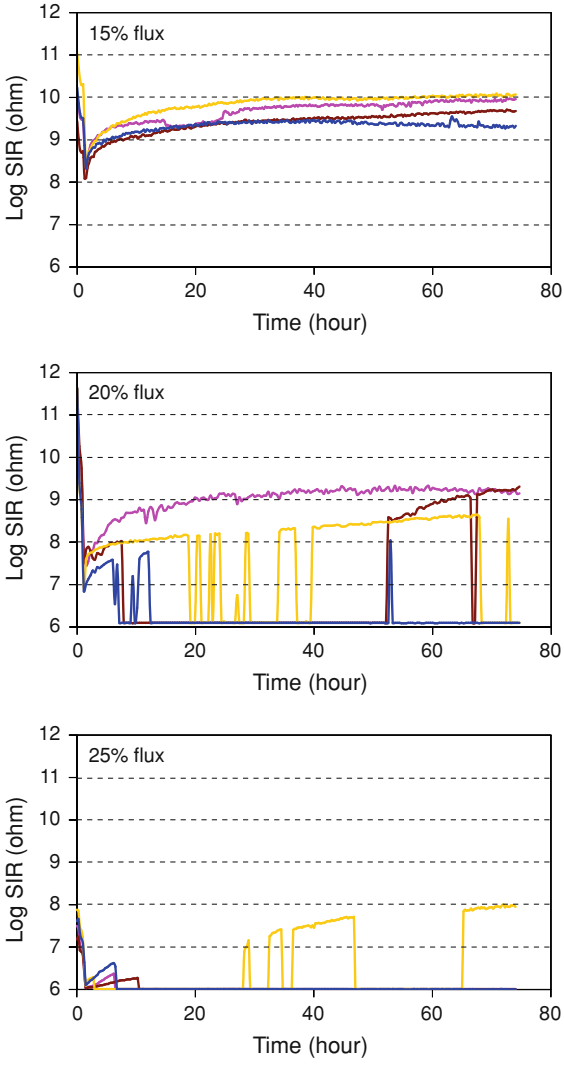


**Fig. 4.11** SIR results from SnPb boards with three concentrations of flux

Sn, for some dendrites there was higher Ag and Cu. These results do not suggest a particular sensitivity to Ag, further work is need here to substantiate earlier work at NPL [14] that Ag migration is an issue when Ni is present. A contributory factor suggested by Yu [15] is the formation of inter-metallic compounds in the solder alloy that prevent Ag migration. For Sn finish, dendrites were 100% Sn.

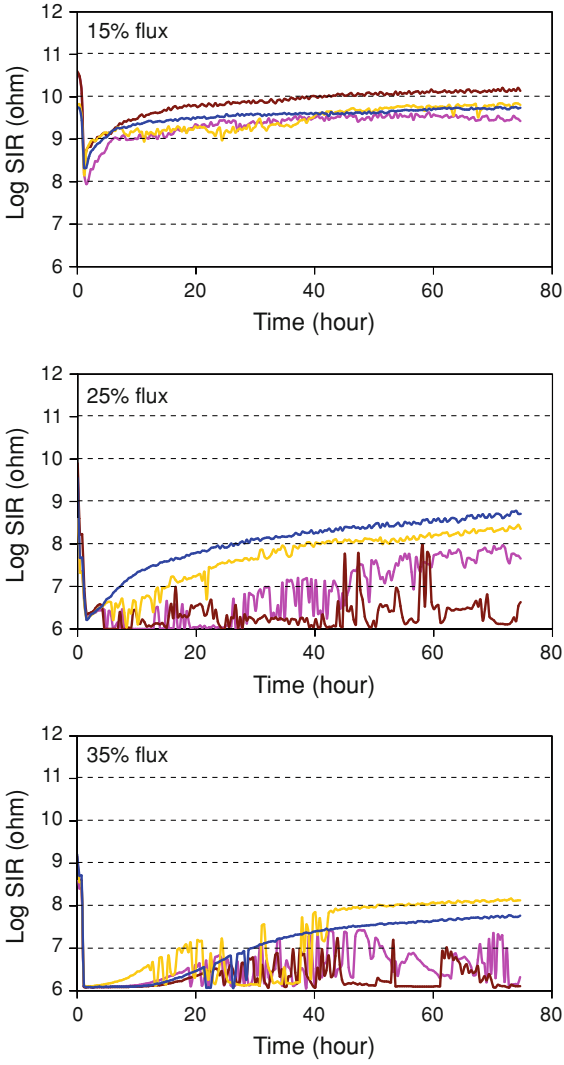


**Fig. 4.12** SIR results from SAC boards with three concentrations of flux

## 4.4 Discussion

### *4.4.1 Ionic Resistance for Different Board Finishes*

An aim of EI measurements is to evaluate the metal corrosion rate at the anode, but for our test system, the impedance attributed to corrosion process $\boldsymbol{R_p}$ is not easy to

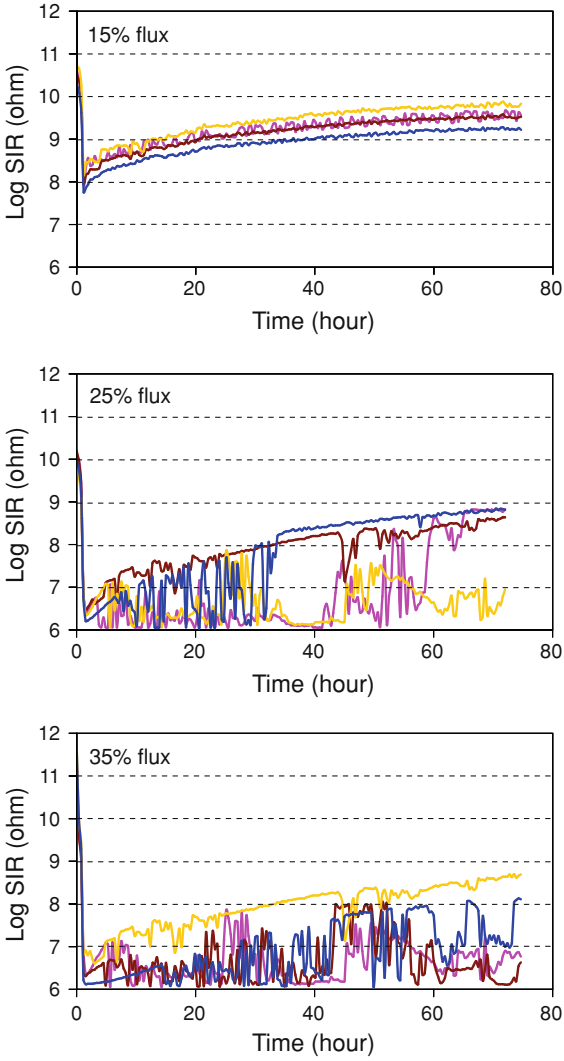


**Fig. 4.13** SIR results from Sn boards with three concentrations of flux

interpret, due to the high ionic resistance between the two electrodes. The different finished boards were similarly contaminated, if metal corrosion was not significant, the ionic resistance between two electrodes will be the most significant part of the overall impedance. Therefore, under these circumstances, the $\boldsymbol{R_c}$ should be the same for different board finishes. The difference on ionic resistance $\boldsymbol{R_c}$ on different board finishes must be due to the metal corrosion. Metal corrosion can affect $\boldsymbol{R_c}$ in two ways: Firstly, if the metal has high corrosion rate, more metal ions

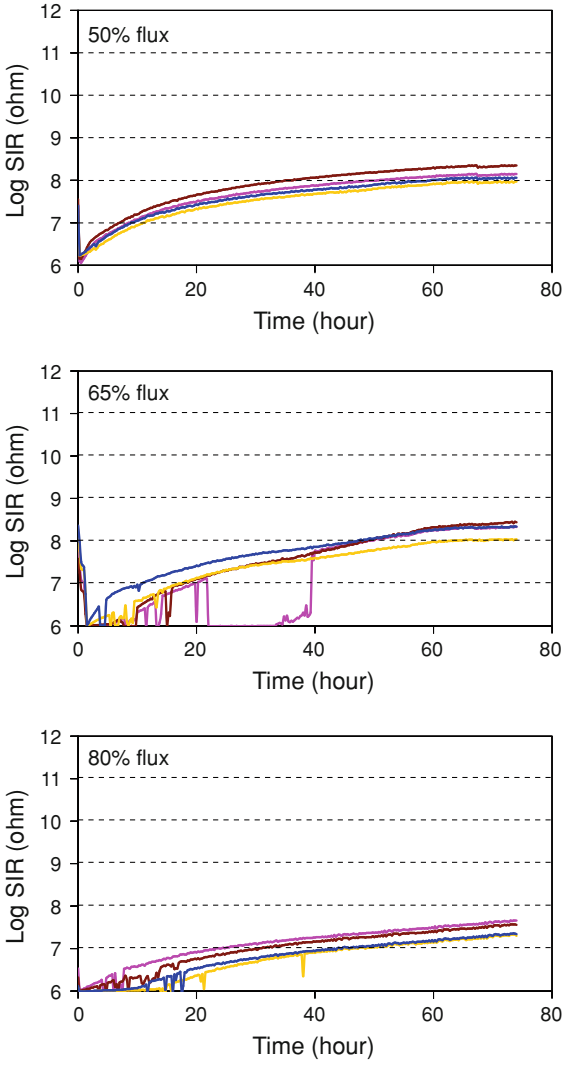


**Fig. 4.14** SIR results from Cu boards with three concentrations of flux

**Table 4.3** The FCPD on different finish boards

| Board finish | FCPD (% in IPA) |
|---|---|
| ENIG | 10 |
| SnPb | 20 |
| SAC | 25 |
| Sn | 25 |
| Cu | 65 |

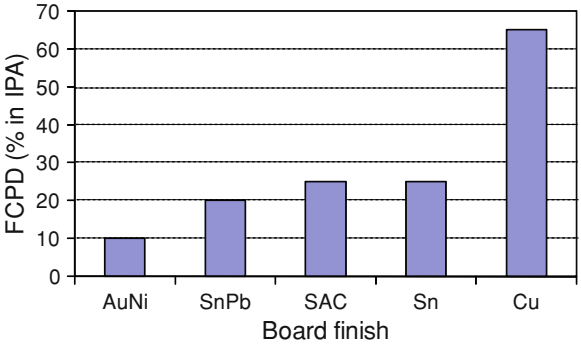


**Fig. 4.15** THE FCPD on different finish boards

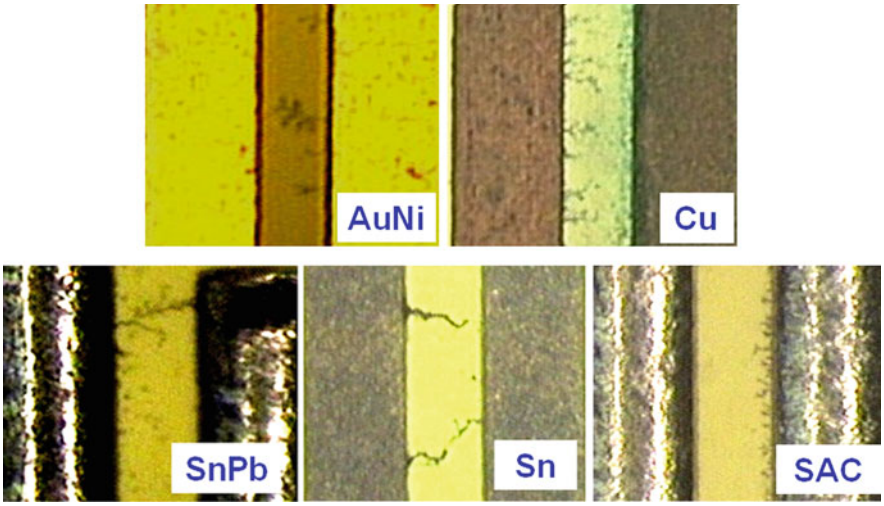


**Fig. 4.16** Optical images for dendrite formed on different board finishes

can be produced from anode into the electrolyte lowing ionic resistance $\boldsymbol{R_c}$ of the system. Secondly, if the corrosion products metal hydroxide has high solubility, corroded metal ions will stay in electrolyte and contribute to conduction process lowing $\boldsymbol{R_c}$. Therefore, although $\boldsymbol{R_c}$ is not a direct measure of metal corrosion rate, it is a function of the metal corrosion rate and metal hydroxide solubility.

### *4.4.2 Effect of Ionic Resistance on Dendrite Formation*

As discussed in the previous section, ionic resistance reflects a combination of the metal corrosion rate and solubility of the metal hydroxide. In this section, the

**Table 4.4** Dendrite formed on an ENIG-finished board

| Spectrum | Ni | Au |
|---|---|---|
| 1 | 100.0 | |
| 2 | 92.8 | 7.1 |
| 3 | 100.0 | |
| 4 | 100.0 | |
| 5 | 100.0 | |

**Table 4.5** Dendrite formed on a copper-finished board

| Spectrum | Cu |
|---|---|
| 1 | 100.0 |
| 2 | 100.0 |
| 3 | 100.0 |
| 4 | 100.0 |
| 5 | 100.0 |

**Table 4.6** Dendrite formed on a SnPb-finished board

| Spectrum | Sn | Pb |
|---|---|---|
| 1 | 17.1 | 82.9 |
| 2 | 56.2 | 43.8 |
| 3 | 26.2 | 73.8 |
| 4 | 16.3 | 83.7 |
| 5 | 32.3 | 67.7 |

**Table 4.7** Dendrite formed on a SAC-finished board

| Spectrum | Cu | Ag | Sn |
|---|---|---|---|
| 1 | 0.5 | 3.7 | 95.8 |
| 2 | | 7.9 | 92.1 |
| 3 | 5.6 | | 93.4 |
| 4 | 0.9 | 2.3 | 96.8 |
| 5 | | 4.5 | 95.5 |
| 6 | 2.5 | 3.1 | 94.4 |

**Table 4.8** Dendrite formed on a Sn-finished board

| Spectrum | Sn |
|---|---|
| 1 | 100 |
| 2 | 100 |
| 3 | 100 |
| 4 | 100 |
| 5 | 100 |
| 6 | 100 |

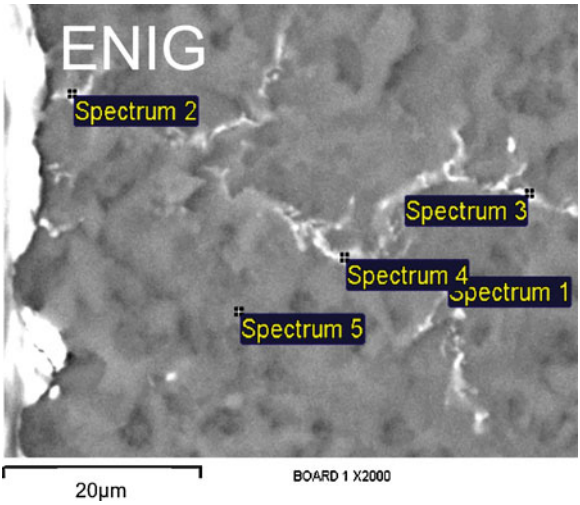


**Fig. 4.17** Dendrite formed on an ENIG-finished board

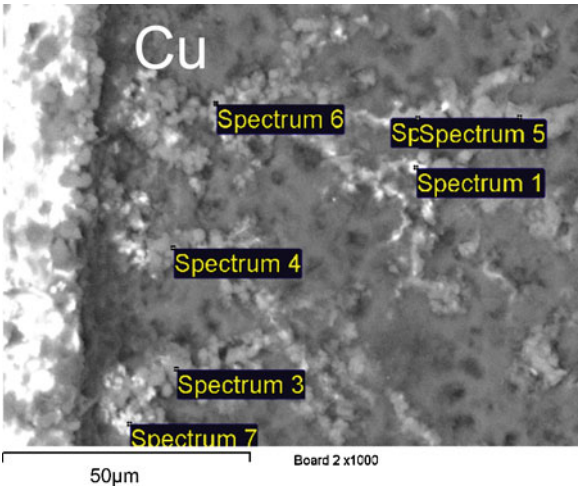


**Fig. 4.18** Dendrite formed on a Cu-finished board

effect of the metal corrosion rate and solubility of the metal hydroxide on dendrite formation are discussed with the three steps involved for dendrite formation.

Dendrite formation can be considered as three-step process as mentioned in the introduction, the most important step is metal ion dissolution at the anode, and a higher corrosion rate will produce more metal ions to migrate from the anode to form dendrites. The metal ion produced at the anode must be able to migrate to the cathode without being precipitated as insoluble compounds; hence, the solubility of metal hydroxide will also affect the metal migration.

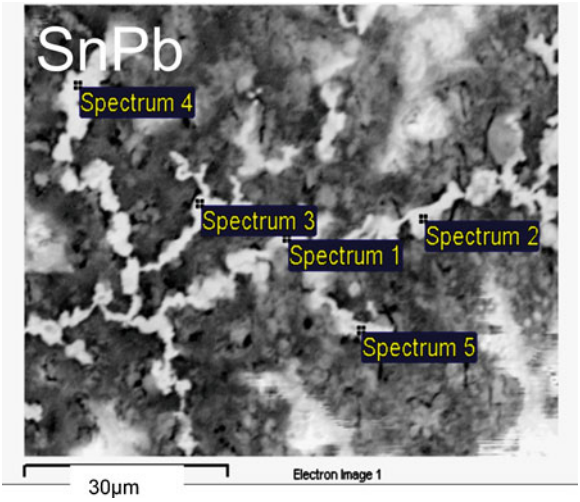


**Fig. 4.19** Dendrite formed on a SnPb-finished board

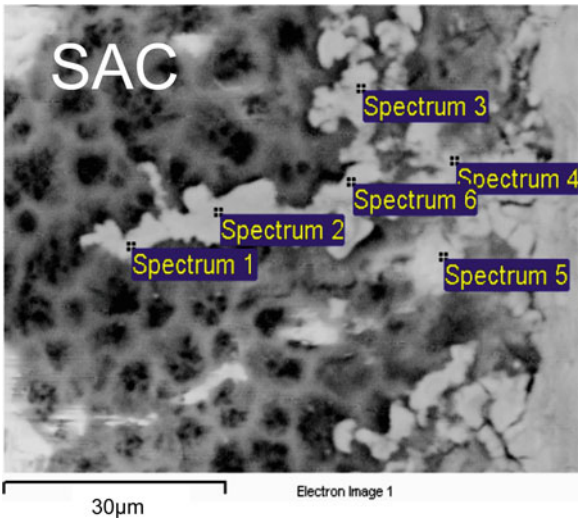


**Fig. 4.20** Dendrite formed on a SAC-finished board

With SIR testing when 5 V DC is applied to the test comb, thermodynamically metal dissolution at the anode will dominate the anodic reactions. At the cathode, hydrogen and oxygen reduction will be preferable reactions, as there is sufficient $H^+$ from flux residues and $O_2$ in the thin water film. Metal ion deposition may not occur unless the over-potential is sufficiently high since the metal ion concentration may be low due to limited dissolution at the anode. Previous work also found that a minimum cathodic over-potential was required for the appearance and propagation of dendrite [7]. The voltage value, 5 V, between the anode and cathode would

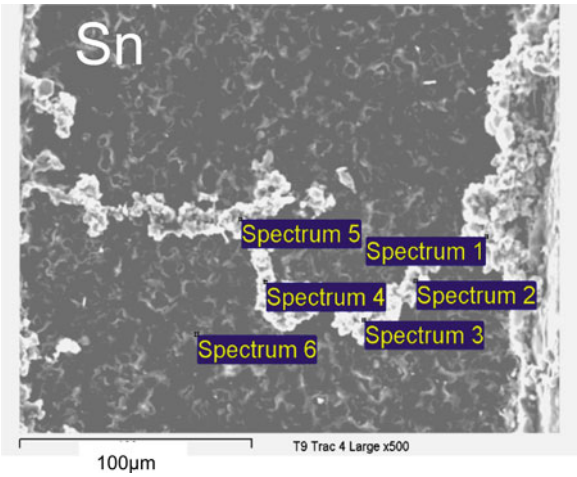


**Fig. 4.21** Dendrite formed on a Sn-finished board

normally be considered to be high for an electrochemical process in solution. However, the electrolyte on the comb is a thin water film, and hence, there is a significant voltage drop across the inter-electrode gap $\boldsymbol{R}_{\mathbf{C}}$. Therefore, the activation over-potential at the electrodes is very small and depends on the $\boldsymbol{R}_{\mathbf{C}}$ value. If system has low $\boldsymbol{R}_{\mathbf{C}}$, then more voltage is dropped at the electrodes and a higher over-potential is achieved. With a higher over-potential at the cathode, there is an increased the ability for metal ion deposition.

Furthermore, a high over-potential at the anode accelerates metal dissolution, and in turn, more metal ions will be produced in the electrolyte. Thus, a system with low $\boldsymbol{R}_{\mathbf{C}}$, both the metal ion concentration and the cathodic over-potential will be high and help to promote metal ion deposition at the cathode. Therefore, ionic resistance $\boldsymbol{R}_{\mathbf{C}}$ is a very important indicator on dendrite formation for the system.

### *4.4.3 EI Measurement to Predict Dendrite Formation*

The ranking on propensity to form dendrite for five studied metals from SIR measurements demonstrates an inverse correlation with ionic resistance ($\boldsymbol{R}_{\mathbf{C}}$) interpreted from the EI results. Therefore, $\boldsymbol{R}_{\mathbf{C}}$ can be used to predict the propensity of the studied metals to form dendrite. The EI measurements use a small amplitude AC single, and the technique itself does not actually promote dendrites. Hence, this predictive capability could be developed into a non-destructive fast test method.

The higher propensity to form dendrite on SnPb-finished board compared with SAC- and Sn-finished board is due to its low ionic resistance, which was probably caused by high corrosion rate of Pb in SnPb solder alloy, or, and high solubility of $Pb(OH)_2$. This was supported by the EDX analysis of the dendrites showing high

Pb content. Low propensity of lead-free solders implies that the reliability of the circuit will be improved using lead-free solders over a SnPb solder. This will not always be necessarily true, because high temperature soldering process and different metallurgy require more active fluxes for lead-free solder; hence, there is the potential of leaving more flux residues on the circuit. The dendrite formation strongly depends on the level of flux residues, as the SIR results in 3.3, and discussed in previous report [14]. The propensities to form dendrites in lead-free solders, SAC and Sn, are likely to be similar and dominated by the corrosion of Sn, the main constituent in these alloys.

Comparing two PCB finishes of Cu and ENIG, the low propensity to form dendrite for the Cu finish, compared to the ENIG finish, can be attributed to the low corrosion rate and solubility of $Cu(OH)_2$. The low solubility of $Cu(OH)_2$ was evidenced by some green corrosion products observed around the anode in Fig. 4.16.

## 4.5 Conclusions

Electrochemical Impedance measurements have been made of three solders and two PCB finish materials. Effect of metal corrosion on reliability of circuit (dendrite formation) has been investigated using SIR measurement. In developing the impedance technique, results were compared with those taken with SIR. The corrosion conditions were manipulated so that dendrite formation occurred, and the dendrite composition was confirmed with EDX. The dominant conduction process for dendrite formation has been identified.

EI results were recorded over a wide range frequency on comb test pattern, as typically used in the SIR technique. This allowed the ionic resistance $\boldsymbol{R_C}$ between two electrodes to be separated from the overall impedance of the system $\boldsymbol{R_{T(0.01)}}$. $\boldsymbol{R_C}$ was found to be dependent on the metal corrosion rate and solubility of the metal hydroxide. The ranking from the highest to the lowest in terms of the ionic resistance is Cu > Sn ≈ SAC > SnPb > ENIG.

The relative propensity for dendrite formation assessed using SIR measurement demonstrates an inverse correlation with ionic resistance, $\boldsymbol{R_C}$, interpreted from the EI results. In a system with low $\boldsymbol{R_C}$, a significant amount of metal ion migration occurs, resulting in dendrite formation and probable short circuit. Hence, from these results, the $\boldsymbol{R_C}$ value could be interpreted in the relative likelihood for dendrites to form and so the reliability of electronic assemblies. Since the EI technique only applies a 50 mV AC signal, and a scan takes less than one hour, the $\boldsymbol{R_C}$ measurement can be considered to be a fast and method non-destructive.

Dendrite formation is a complex electrochemical processes, dependent on both the metal corrosion rate and the solubility of metal hydroxide. The high propensity to form dendrite of a SnPb solder compared with a SAC solder and Sn is due to high corrosion rate of Pb in SnPb solder alloy, or, and high solubility of $Pb(OH)_2$. Therefore, under the same contamination conditions, an electronic circuit will be

more reliable if soldered with lead-free solders. Furthermore a Cu-finished PCB will be less likely to form dendrites compared to the ENIG finish due to its low corrosion rate and low solubility of $Cu(OH)_2$.

**Acknowledgments** The work was carried out as part of a project, Measure Electrochemical Corrosion of Lead-Free Process Residues in Electronic Assemblies, in the Processing Programme of the UK Department of Trade and Industry.

## References

1. Chan HA (1996) Surface insulation resistance methodology for today's manufacturing technology. IEEE Trans Compon Packaging Manuf Technol Part C 19(4):300–307
2. Hunt C, Zou CL (1999) The impact of temperature and humidity condition on surface insulation resistance values for various fluxes. Soldering Surf Mt Technol 11(1):21–24
3. Zou CL, Hunt C (1999) The effect of test voltage, test pattern and board finish on surface insulation resistance (SIR) measurements for various fluxes. NPL Report CMMT(A)222
4. Harsanyi G (1995) Electrochemical process resulting in migrated short failures in microcircuit. IEEE Trans Compon Packaging Manuf Technol Part A 18(3):602–610
5. Zou CL, Hunt C (2006) Electrochemical behavior of solder alloy. NPL Report DEPC-MPR (PAPER) 040 September
6. Steppan JJ, Roth JA, Hall LC, Jeanotte DA, Carbone SP (1987) A review of corrosion failure mechanisms during accelerated test. J Electrochem Soc 134:175–190
7. Zamanzadeh M (1990) Electrochemical examination of dendrite growth on electronic devices in HCl electrolytes. Corrosion 46(8):665–671
8. Yang S (2007) Failure model for silver electrochemical migration. IEEE Trans Divice Mater Reliab 7(1):188–196
9. Brusic V, Dimilia DD, Macinnes R (1991) Corrosion of led, tin, and their alloys. Corrosion 47(7):509–518
10. Mohanty US, Lin KL (2007) Electrochemical corrosion study on Sn-XAg-0.5Cu alloys in 3.5% NaCl solution. J Mater Res 22(9):2573–2581
11. Beccaria AM, Mor ED, Bruno G, Poggi G (1982) Corrosion of lead in sea water. Br Corros J 17(2):87–91
12. Zou CL, Hunt C (2009) Characterization of the conduction mechanisms in adsorbed electrolyte layers on printed circuit boards using AC impedance. J Electrochem Soc 156(1):C5–C15
13. Takahashi KM (1991) Conduction paths and mechanisms in FR-4 epoxy/glass composite printed wiring boards. J Electrochem Soc 138(6):1587–1593
14. Zou CL, Hunt C (2007) Susceptibility of lead-free system to electrochemical migration. NPL Report MAT1
15. Yu DQ (2006) Electrochemical migration of SnPb and Lead free solder alloys under distilled water. J Mater Sci Mater Electron 17:219–227. doi:10.1007/s10854-006-6764-0